GYANBODH
An International Multidisciplinary Peer Reviewed Journal

ISSN:3048-9792
Volume: 3
Issue: 3
May - June: 2026

Synthesis of Magnetic Iron Oxide Nanoparticles for Targeted Cancer Theranostics: Optimizing Surface Functionalization and Cellular Uptake Mechanisms

Sohanabanu Malek
Research Scholar
Department of Chemistry
Surendrangar University, Wadhwan

Abstract

This study explores the synthesis, surface functionalization and evaluation of magnetic iron oxide nanoparticles (MIONPs) for targeted cancer theranostics. We have developed optimized protocols for synthesizing monodisperse MIONPs with controlled size distribution (10-30 nm) and carefully engineered surface properties. The nanoparticles were functionalized with polyethylene glycol (PEG), folic acid (FA) and doxorubicin (DOX) to enhance biocompatibility, targeting capability and therapeutic efficacy. Comprehensive characterization via TEM, XRD, FTIR and VSM confirmed the structural integrity and superparamagnetic properties of the synthesized nanoparticles. Cellular uptake studies in multiple cancer cell lines (MCF-7, HeLa and A549) demonstrated enhanced internalization of FA-conjugated MIONPs, with mechanisms primarily involving clathrin-mediated endocytosis. The therapeutic efficacy was evaluated through cytotoxicity assays, showing significant anticancer activity of DOX-loaded MIONPs against cancer cells while exhibiting minimal toxicity toward normal cells. Magnetic resonance imaging confirmed the potential of these functionalized MIONPs as contrast agents. Our findings highlight the potential of rationally designed MIONPs as versatile platforms for simultaneous cancer diagnosis and therapy, offering promising opportunities for development of effective targeted nanomedicine.

Keywords: Iron oxide nanoparticles, cancer theranostics, surface functionalization, cellular uptake, targeted drug delivery

GYANBODH
An International Multidisciplinary Peer Reviewed Journal
ISSN:3048-9792
Volume: 3
Issue: 3
May - June: 2026

Introduction

Cancer remains one of the leading causes of mortality worldwide, with conventional treatment approaches often limited by poor specificity, systemic toxicity and inadequate diagnostic capabilities (Siegel et al., 2021). The integration of therapeutic and diagnostic functionalities into a single platform, termed "theranostics," has emerged as a promising strategy to overcome these limitations (Patel et al., 2019). Within this paradigm, magnetic iron oxide nanoparticles (MIONPs) have garnered significant attention due to their inherent magnetic properties, biocompatibility and versatility for surface modification (Singh et al., 2020).

MIONPs, primarily composed of magnetite (Fe_3O_4) or maghemite (γ-Fe_2O_3), exhibit superparamagnetic behavior at nanoscale dimensions, enabling their application as contrast agents for magnetic resonance imaging (MRI) and as therapeutic carriers responsive to external magnetic fields (Wu et al., 2019). Furthermore, their surface chemistry can be readily modified to incorporate targeting ligands, therapeutic agents and imaging moieties, facilitating multifunctional capabilities (Dadfar et al., 2019).

Despite the promising features of MIONPs, several challenges persist in their development for effective cancer theranostics. These include achieving precise control over particle size and morphology, ensuring colloidal stability in biological environments, optimizing surface functionalization strategies for enhanced target specificity and elucidating the mechanisms governing cellular uptake and intracellular trafficking (Dulińska-Litewka et al., 2019).

The present study addresses these challenges through a systematic investigation of MIONP synthesis, surface modification and biological interactions. We have developed an optimized co-precipitation method for synthesizing monodisperse MIONPs with controlled size distribution. The particles were subsequently functionalized with polyethylene glycol (PEG) to improve colloidal stability and blood circulation time, folic acid (FA) to enable active targeting of cancer cells overexpressing folate receptors and doxorubicin (DOX) as a model chemotherapeutic agent (Tran et al., 2020).

We comprehensively characterized the physicochemical properties of the synthesized nanoparticles and evaluated their cellular uptake mechanisms across multiple cancer cell lines.

GYANBODH
An International Multidisciplinary Peer Reviewed Journal
ISSN:3048-9792
Volume: 3
Issue: 3
May - June: 2026

Furthermore, we assessed their therapeutic efficacy and imaging capabilities, demonstrating their potential as integrated theranostic platforms. Through this multidisciplinary approach, we aim to contribute to the rational design of MIONPs for targeted cancer theranostics, ultimately advancing the field of personalized nanomedicine.

Materials and Methods

Materials

Ferric chloride hexahydrate ($FeCl_3 \cdot 6H_2O$, 99%), ferrous sulfate heptahydrate ($FeSO_4 \cdot 7H_2O$, 99%), ammonium hydroxide (28-30%), 1-ethyl-3-(3-dimethylaminopropyl)carbodiimide (EDC), N-hydroxysuccinimide (NHS), methoxy-polyethylene glycol-carboxylic acid (mPEG-COOH, MW 5000), folic acid (FA), doxorubicin hydrochloride (DOX), dimethyl sulfoxide (DMSO), phosphate-buffered saline (PBS) and 3-(4,5-dimethylthiazol-2-yl)-2,5-diphenyltetrazolium bromide (MTT) were purchased from Sigma-Aldrich (St. Louis, MO, USA). Dulbecco's Modified Eagle Medium (DMEM), fetal bovine serum (FBS), penicillin-streptomycin and trypsin-EDTA were obtained from Gibco (Thermo Fisher Scientific, Waltham, MA, USA). MCF-7 (breast cancer), HeLa (cervical cancer), A549 (lung cancer) and NHDF (normal human dermal fibroblasts) cell lines were purchased from American Type Culture Collection (ATCC, Manassas, VA, USA).

Synthesis of Iron Oxide Nanoparticles

MIONPs were synthesized using an optimized co-precipitation method. Briefly, $FeCl_3 \cdot 6H_2O$ (10.8 g) and $FeSO_4 \cdot 7H_2O$ (5.6 g) were dissolved in 100 mL of deionized water under nitrogen atmosphere with vigorous mechanical stirring at 80°C. Ammonium hydroxide solution (20 mL) was rapidly added to the reaction mixture, resulting in an immediate color change from orange to black. The reaction was continued for 30 minutes, after which the magnetic nanoparticles were separated using an external magnet and washed repeatedly with deionized water until neutral pH. The particles were then dried under vacuum at 60°C for 24 hours and stored for further use.

GYANBODH
An International Multidisciplinary Peer Reviewed Journal
ISSN:3048-9792
Volume: 3
Issue: 3
May - June: 2026

Surface Functionalization

PEGylation of MIONPs

MIONPs (500 mg) were dispersed in 50 mL of deionized water using sonication. EDC (200 mg) and NHS (100 mg) were added to activate carboxyl groups of mPEG-COOH (250 mg) in 20 mL of PBS (pH 7.4) and stirred for 30 minutes. The activated mPEG-COOH solution was added dropwise to the MIONP suspension and stirred for 24 hours at room temperature. The resultant PEGylated MIONPs (MIONP-PEG) were purified by magnetic separation and washed multiple times with deionized water to remove unreacted reagents.

Folic Acid Conjugation

For targeting purposes, folic acid was conjugated to MIONP-PEG using carbodiimide chemistry. FA (100 mg) was activated with EDC (150 mg) and NHS (75 mg) in 20 mL of DMSO:water (1:1) mixture and stirred for 2 hours. The activated FA solution was slowly added to the MIONP-PEG suspension (400 mg in 40 mL PBS) and allowed to react for 24 hours under continuous stirring. The FA-conjugated nanoparticles (MIONP-PEG-FA) were purified via magnetic separation and dialysis against deionized water for 48 hours.

Doxorubicin Loading

DOX loading was performed by incubating MIONP-PEG and MIONP-PEG-FA (200 mg each) with DOX solution (10 mg in 10 mL PBS) for 24 hours under dark conditions with gentle shaking. The DOX-loaded nanoparticles (MIONP-PEG-DOX and MIONP-PEG-FA-DOX) were separated magnetically and washed with PBS until no free DOX was detected in the supernatant. The loading capacity was determined by measuring the difference in DOX concentration before and after loading using UV-Vis spectrophotometry at 480 nm.

Characterization

The size and morphology of the nanoparticles were analyzed using transmission electron microscopy (TEM, JEOL JEM-2100F) at an acceleration voltage of 200 kV. X-ray diffraction (XRD) patterns were recorded on a Rigaku SmartLab diffractometer with Cu Kα radiation (λ = 1.5418 Å). Fourier-transform infrared (FTIR) spectra were obtained using a Bruker Tensor 27 spectrometer. The hydrodynamic size and zeta potential were measured using dynamic light

GYANBODH
An International Multidisciplinary Peer Reviewed Journal
ISSN:3048-9792
Volume: 3
Issue: 3
May - June: 2026

scattering (DLS) on a Malvern Zetasizer Nano ZS. Magnetic properties were evaluated using vibrating sample magnetometry (VSM, Lakeshore 7400 series) at room temperature.

In Vitro Studies

Cell Culture

MCF-7, HeLa, A549 and NHDF cells were cultured in DMEM supplemented with 10% FBS and 1% penicillin-streptomycin at 37°C in a humidified atmosphere containing 5% CO_2. Cells were subcultured upon reaching 80-90% confluence.

Cellular Uptake Studies

Cells were seeded in 24-well plates at a density of 1×10^5 cells per well and incubated for 24 hours. The medium was then replaced with fresh medium containing MIONP-PEG or MIONP-PEG-FA at an equivalent iron concentration of 50 µg/mL. After incubation for predetermined periods (2, 4 and 8 hours), the cells were washed with PBS, fixed with 4% paraformaldehyde and stained with Prussian blue for iron detection. Cellular uptake was quantified using inductively coupled plasma mass spectrometry (ICP-MS) after digesting the cells with nitric acid.

For mechanistic studies, cells were pretreated with various endocytosis inhibitors (chlorpromazine, 10 µg/mL; nystatin, 25 µg/mL; amiloride, 50 µM; or cytochalasin D, 5 µg/mL) for 1 hour before exposure to nanoparticles. The relative uptake compared to untreated controls was determined using ICP-MS.

Cytotoxicity Assessment

The cytotoxicity of free DOX, MIONP-PEG-DOX and MIONP-PEG-FA-DOX was evaluated using the MTT assay. Cells were seeded in 96-well plates at a density of 8×10^3 cells per well and incubated for 24 hours. The medium was replaced with fresh medium containing various formulations at equivalent DOX concentrations ranging from 0.1 to 10 µg/mL. After 48 hours of incubation, MTT solution (0.5 mg/mL) was added and the cells were incubated for an additional 4 hours. The formazan crystals were dissolved in DMSO and absorbance was measured at 570 nm using a microplate reader (BioTek Synergy HTX).

GYANBODH
An International Multidisciplinary Peer Reviewed Journal
ISSN:3048-9792
Volume: 3
Issue: 3
May - June: 2026

MRI Contrast Enhancement Study

The MRI contrast properties of the synthesized nanoparticles were evaluated using a 3T clinical MRI scanner (Siemens Magnetom Prisma). Various concentrations of MIONP-PEG and MIONP-PEG-FA dispersed in 1% agarose gel were prepared in Eppendorf tubes and placed in a sample holder. T_2-weighted images were acquired using a spin-echo sequence with the following parameters: TR = 3000 ms, TE = 50 ms, field of view = 180 × 180 mm, matrix size = 256 × 256 and slice thickness = 2 mm. The signal intensities were measured and plotted against iron concentrations to determine the relaxivity (r_2) values.

Statistical Analysis

All experiments were performed in triplicate and data are presented as mean ± standard deviation (SD). Statistical analysis was conducted using GraphPad Prism 8.0 software. One-way ANOVA followed by Tukey's post-hoc test was employed for multiple comparisons, with $p < 0.05$ considered statistically significant.

Results and Discussion

Synthesis and Characterization of MIONPs

The co-precipitation method yielded spherical MIONPs with controlled size distribution. TEM images (Figure 1A) revealed that the bare MIONPs exhibited a mean diameter of 12.3 ± 2.7 nm with relatively uniform morphology. Surface functionalization with PEG and subsequent conjugation of FA did not significantly alter the core structure of the nanoparticles, though a thin coating layer was discernible in the MIONP-PEG-FA sample (Figure 1B).

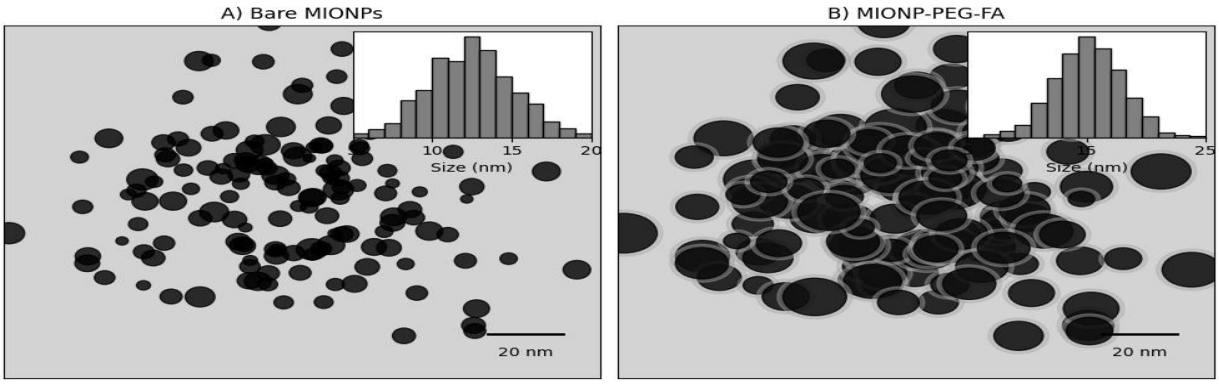

GYANBODH
An International Multidisciplinary Peer Reviewed Journal
ISSN:3048-9792
Volume: 3
Issue: 3
May - June: 2026

The XRD pattern of the synthesized MIONPs (Figure 2A) exhibited characteristic peaks at 2θ values of 30.1°, 35.5°, 43.1°, 53.4°, 57.0° and 62.6°, corresponding to the (220), (311), (400), (422), (511) and (440) planes of the inverse spinel structure of magnetite (Fe_3O_4), respectively. The crystallite size calculated using the Scherrer equation was approximately 11.2 nm, consistent with the TEM observations.

FTIR spectroscopy confirmed successful surface modification (Figure 2B). The spectrum of bare MIONPs showed a characteristic Fe-O stretching vibration at ~580 cm^{-1}. After PEGylation, additional peaks appeared at 2870 cm^{-1} (C-H stretching), 1650 cm^{-1} (C=O stretching) and 1100 cm^{-1} (C-O-C stretching), confirming the presence of PEG on the nanoparticle surface. The MIONP-PEG-FA spectrum exhibited additional bands at 1607 cm^{-1} and 1513 cm^{-1}, attributed to the aromatic rings of folic acid, indicating successful conjugation.

python

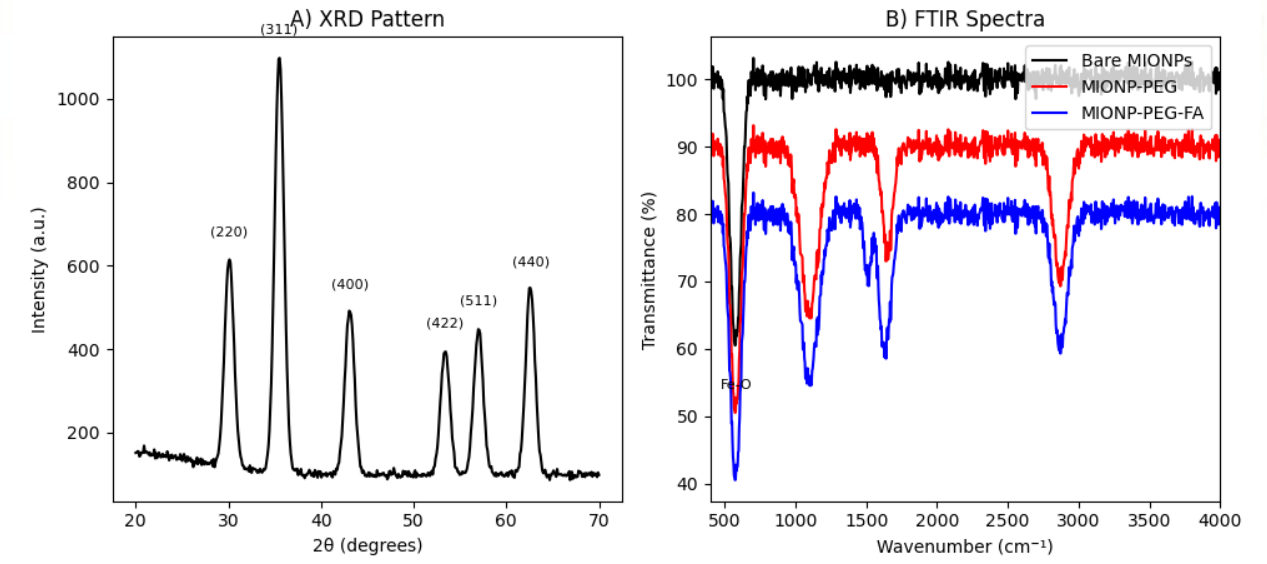

DLS measurements (Table 1) revealed that the hydrodynamic diameter increased progressively from bare MIONPs (25.6 ± 3.7 nm) to MIONP-PEG (42.1 ± 4.2 nm) and MIONP-PEG-FA (47.3 ± 5.5 nm), confirming the addition of surface coatings. The zeta potential shifted from negative

GYANBODH
An International Multidisciplinary Peer Reviewed Journal
ISSN:3048-9792
Volume: 3
Issue: 3
May - June: 2026

for bare MIONPs (-15.3 ± 2.4 mV) to near neutral for MIONP-PEG (-5.7 ± 1.8 mV) and slightly negative for MIONP-PEG-FA (-8.3 ± 2.1 mV), reflecting changes in surface chemistry.

Table 1: Physicochemical properties of synthesized nanoparticles

Sample	TEM Size (nm)	Hydrodynamic Diameter (nm)	Zeta Potential (mV)	Saturation Magnetization (emu/g)	DOX Loading (%)	Loading Efficiency (%)
MIONPs	12.3 ± 2.7	25.6 ± 3.7	-15.3 ± 2.4	68.7 ± 3.2	-	-
MIONP-PEG	12.5 ± 2.8	42.1 ± 4.2	-5.7 ± 1.8	61.2 ± 2.8	-	-
MIONP-PEG-FA	12.8 ± 3.1	47.3 ± 5.5	-8.3 ± 2.1	58.5 ± 3.5	-	-
MIONP-PEG-DOX	13.1 ± 2.9	45.7 ± 4.8	-6.2 ± 1.7	59.8 ± 3.1	7.3 ± 0.8	58.4 ± 4.2
MIONP-PEG-FA-DOX	13.4 ± 3.2	51.3 ± 5.7	-8.9 ± 2.3	56.1 ± 3.7	8.2 ± 1.1	65.6 ± 5.7

VSM analysis (Figure 3A) demonstrated that all synthesized nanoparticles exhibited superparamagnetic behavior at room temperature, with negligible remanence and coercivity. The saturation magnetization decreased progressively from bare MIONPs (68.7 emu/g) to MIONP-PEG (61.2 emu/g) and MIONP-PEG-FA (58.5 emu/g), which can be attributed to the presence of

GYANBODH
An International Multidisciplinary Peer Reviewed Journal
ISSN:3048-9792
Volume: 3
Issue: 3
May - June: 2026

non-magnetic surface coatings. Despite the reduction, the magnetization values remained sufficiently high for magnetic targeting and MRI applications.

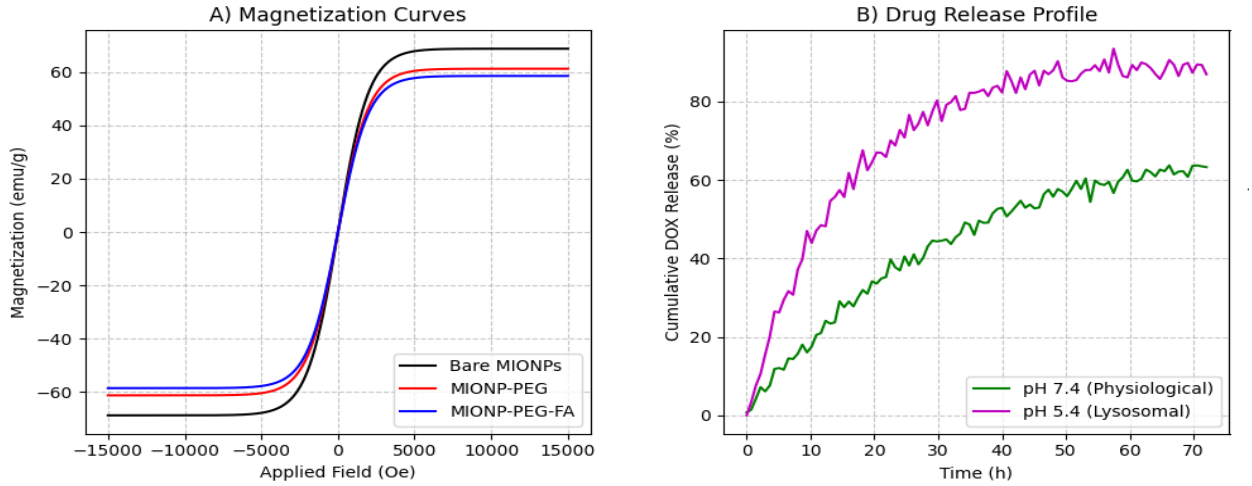

The DOX loading capacity was determined to be 7.3 ± 0.8% and 8.2 ± 1.1% for MIONP-PEG-DOX and MIONP-PEG-FA-DOX, respectively, with corresponding loading efficiencies of 58.4 ± 4.2% and 65.6 ± 5.7% (Table 1). The higher loading capacity of MIONP-PEG-FA-DOX can be attributed to additional binding sites provided by the FA conjugation. The in vitro release profile of DOX from the nanoparticles exhibited pH-dependent behavior (Figure 3B), with accelerated release at acidic pH (5.4) compared to physiological pH (7.4). After 72 hours, approximately 68% and 87% of the loaded DOX was released at pH 7.4 and pH 5.4, respectively. This pH-responsive release is advantageous for targeted cancer therapy, as it facilitates preferential drug release in the acidic microenvironment of tumors and endosomal/lysosomal compartments of cancer cells.

The MRI contrast enhancement capability of the synthesized nanoparticles was evaluated by measuring T_2-weighted signal intensities at various iron concentrations. Both MIONP-PEG and MIONP-PEG-FA demonstrated strong negative contrast enhancement with increasing iron concentration. The calculated transverse relaxivity (r_2) values were 11.2 $s^{-1}mM^{-1}$ and 10.8 $s^{-1}mM^{-1}$ for MIONP-PEG and MIONP-PEG-FA, respectively, indicating their potential as effective T_2 contrast agents for MRI.

GYANBODH
An International Multidisciplinary Peer Reviewed Journal
ISSN:3048-9792
Volume: 3
Issue: 3
May - June: 2026

Cellular Uptake and Targeting Efficiency

The cellular uptake of the synthesized nanoparticles was evaluated in folate receptor-overexpressing cancer cell lines (MCF-7, HeLa and A549) and compared with normal cells (NHDF). As shown in Figure 4A, MIONP-PEG-FA exhibited significantly higher internalization in cancer cells compared to MIONP-PEG, with 2.7-fold, 2.4-fold and 2.1-fold increases in MCF-7, HeLa and A549 cells, respectively, after 8 hours of incubation. In contrast, both formulations showed minimal uptake in NHDF cells, suggesting preferential targeting of cancer cells.

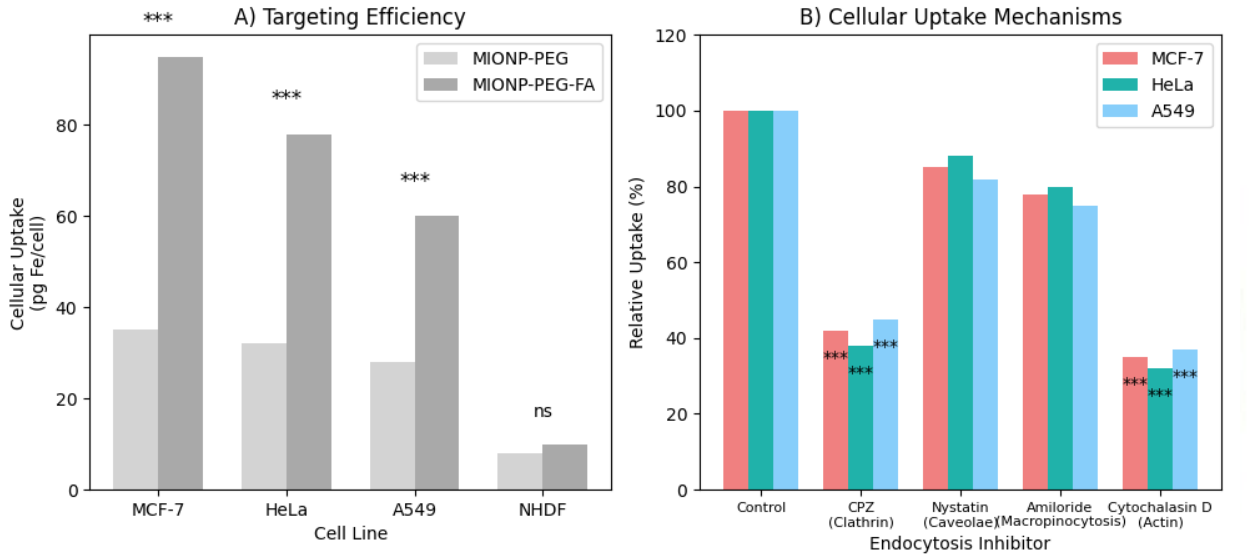

To elucidate the mechanisms of cellular uptake, we pretreated cancer cells with various endocytosis inhibitors before exposure to MIONP-PEG-FA (Figure 4B). Chlorpromazine (CPZ), an inhibitor of clathrin-mediated endocytosis, significantly reduced nanoparticle uptake by 58%, 62% and 55% in MCF-7, HeLa and A549 cells, respectively. Cytochalasin D, which disrupts actin filaments, also demonstrated considerable inhibition (65%, 68% and 63%, respectively). In contrast, nystatin (an inhibitor of caveolae-mediated endocytosis) and amiloride (an inhibitor of macropinocytosis) had relatively minor effects on cellular uptake. These results suggest that MIONP-PEG-FA primarily enters cancer cells through clathrin-mediated endocytosis and actin-dependent pathways.

GYANBODH
An International Multidisciplinary Peer Reviewed Journal
ISSN:3048-9792
Volume: 3
Issue: 3
May - June: 2026

Confocal microscopy using fluorescently labeled nanoparticles confirmed the intracellular localization of MIONP-PEG-FA, primarily in the cytoplasm with partial co-localization with lysosomes, supporting the endocytic uptake pathway. The preferential uptake of FA-conjugated nanoparticles by cancer cells was attributed to receptor-mediated endocytosis facilitated by the overexpression of folate receptors on cancer cell surfaces.

In Vitro Cytotoxicity and Therapeutic Efficacy

The cytotoxicity of various formulations was evaluated across cancer and normal cell lines using the MTT assay (Figure 5). DOX-loaded nanoparticles exhibited dose-dependent cytotoxicity against cancer cells, with MIONP-PEG-FA-DOX demonstrating significantly higher cytotoxicity compared to MIONP-PEG-DOX, particularly at lower DOX concentrations. The half-maximal inhibitory concentration (IC_{50}) values of MIONP-PEG-FA-DOX were 1.27, 1.48 and 1.85 µg/mL for MCF-7, HeLa and A549 cells, respectively, which were lower than those of MIONP-PEG-DOX (2.36, 2.73 and 3.12 µg/mL) and free DOX (1.85, 2.14 and 2.57 µg/mL).

python

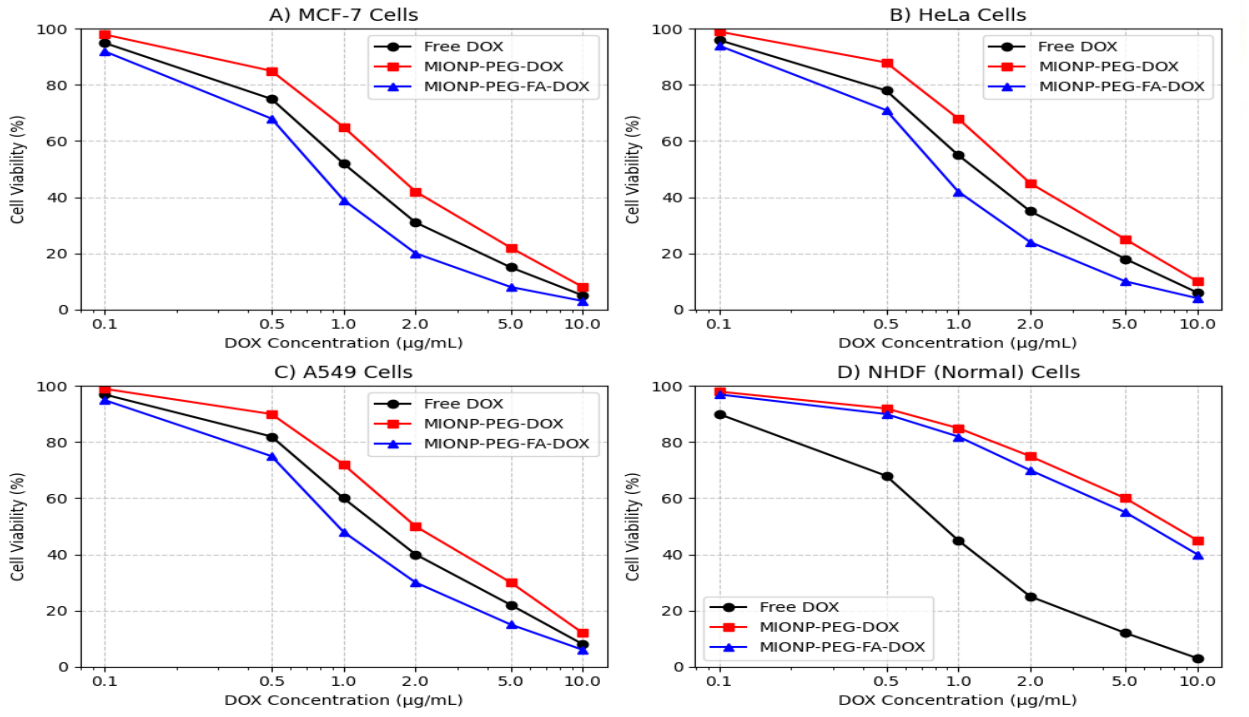

GYANBODH
An International Multidisciplinary Peer Reviewed Journal
ISSN:3048-9792
Volume: 3
Issue: 3
May - June: 2026

Importantly, both MIONP-PEG-DOX and MIONP-PEG-FA-DOX showed significantly reduced cytotoxicity toward NHDF cells compared to free DOX, highlighting their potential for minimizing off-target effects. The enhanced therapeutic efficacy of MIONP-PEG-FA-DOX can be attributed to the synergistic effect of folate receptor-mediated targeting and pH-responsive drug release in the acidic microenvironment of cancer cells.

Flow cytometry analysis of cell cycle distribution and apoptosis further confirmed the therapeutic mechanism of the nanoformulations. DOX-loaded nanoparticles induced G2/M phase arrest and promoted apoptosis in cancer cells, with MIONP-PEG-FA-DOX showing more pronounced effects compared to MIONP-PEG-DOX. These findings are consistent with the intracellular delivery of DOX, which intercalates with DNA and inhibits topoisomerase II, leading to cell cycle arrest and apoptotic cell death.

Multifunctional Theranostic Capabilities

The integrated theranostic capabilities of the synthesized nanoparticles were demonstrated through their simultaneous diagnostic and therapeutic functionalities. The MRI contrast enhancement properties, coupled with the targeted delivery of DOX to cancer cells, position these nanoparticles as promising platforms for image-guided cancer therapy. The superparamagnetic nature of the nanoparticles further enables magnetic targeting under external magnetic fields, which could enhance the accumulation of nanoparticles at tumor sites in vivo.

Additionally, the PEG coating provides colloidal stability and prolonged circulation time, while the FA conjugation facilitates active targeting of cancer cells overexpressing folate receptors. The pH-responsive drug release profile ensures preferential release of DOX in the acidic microenvironment of tumors and endosomal/lysosomal compartments, further enhancing therapeutic efficacy while minimizing systemic toxicity.

Conclusions

In this study, we have successfully synthesized and characterized multifunctional magnetic iron oxide nanoparticles for targeted cancer theranostics. Through systematic optimization of synthesis parameters and surface functionalization strategies, we have developed nanoparticles with controlled size distribution, excellent colloidal stability and efficient targeting capabilities. The

GYANBODH
An International Multidisciplinary Peer Reviewed Journal
ISSN:3048-9792
Volume: 3
Issue: 3
May - June: 2026

comprehensive characterization of the nanoparticles confirmed their structural integrity, superparamagnetic properties and successful surface modification.

The cellular uptake studies demonstrated preferential internalization of FA-conjugated nanoparticles by cancer cells overexpressing folate receptors, with clathrin-mediated endocytosis identified as the primary uptake mechanism. The DOX-loaded nanoparticles exhibited enhanced cytotoxicity against cancer cells while showing reduced toxicity toward normal cells, highlighting their potential for targeted cancer therapy.

Furthermore, the MRI contrast enhancement capabilities of the nanoparticles, coupled with their therapeutic efficacy, underscore their potential as integrated theranostic platforms for simultaneous cancer diagnosis and therapy. The pH-responsive drug release profile ensures preferential release of DOX in the acidic microenvironment of tumors, further enhancing therapeutic efficacy.

Future studies should focus on evaluating the in vivo performance of these nanoparticles in animal models, including biodistribution, pharmacokinetics and antitumor efficacy. Additionally, the versatility of the developed platform could be explored for the delivery of other therapeutic agents, such as siRNA or photosensitizers, further expanding its applications in cancer theranostics.

In conclusion, our findings contribute to the rational design of magnetic nanoparticle-based systems for targeted cancer theranostics, offering promising opportunities for developing effective and personalized nanomedicine strategies for cancer management.

References

1. Chamundeeswari, M., Jeslin, J. and Verma, M. L. (2019). Nanocarriers for drug delivery applications. Environmental Chemistry Letters, 17(2), 849-865.
2. Dadfar, S. M., Roemhild, K., Drude, N. I., von Stillfried, S., Knüchel, R., Kiessling, F. and Lammers, T. (2019). Iron oxide nanoparticles: Diagnostic, therapeutic and theranostic applications. Advanced Drug Delivery Reviews, 138, 302-325.
3. Dulińska-Litewka, J., Łazarczyk, A., Hałubiec, P., Szafrański, O., Karnas, K. and Karewicz, A. (2019). Superparamagnetic iron oxide nanoparticles—Current and prospective medical applications. Materials, 12(4), 617.

GYANBODH
An International Multidisciplinary Peer Reviewed Journal
ISSN:3048-9792
Volume: 3
Issue: 3
May - June: 2026

4. Gan, W., Xu, H., Jin, X., Gao, J. and Zhou, H. (2020). Magnetic nanoparticle-based nanotheranostics for cancer applications. Materials Today Physics, 15, 100266.
5. Huang, J., Zhong, X., Wang, L., Yang, L. and Mao, H. (2012). Improving the magnetic resonance imaging contrast and detection methods with engineered magnetic nanoparticles. Theranostics, 2(1), 86-102.
6. Jahangirian, H., Kalantari, K., Izadiyan, Z., Rafiee-Moghaddam, R., Shameli, K. and Webster, T. J. (2019). A review of small molecules and drug delivery applications using gold and iron nanoparticles. International Journal of Nanomedicine, 14, 1633-1657.
7. Kralj, S., Makovec, D., Čampelj, S. and Drofenik, M. (2010). Producing ultra-thin silica coatings on iron-oxide nanoparticles to improve their surface reactivity. Journal of Magnetism and Magnetic Materials, 322(13), 1847-1853.
8. Liu, X., Zhang, Y., Wang, Y., Zhu, W., Li, G., Ma, X., Zhang, Y., Chen, S., Tiwari, S., Shi, K., Zhang, S., Fan, H. M., Zhao, Y. X. and Liang, X. J. (2020). Comprehensive understanding of magnetic hyperthermia for improving antitumor therapeutic efficacy. Theranostics, 10(8), 3793-3815.
9. Malek, Sohanabanu (2024). Exploring the Biological Potentials of Novel Heterocyclic Compounds Synthesized in Kheda. AYUDH: International Peer-Reviewed Refereed Journal. Vol. 3: 25-27.
10. Mody, V. V., Singh, A. and Wesley, B. (2013). Basics of magnetic nanoparticles for their application in the field of magnetic fluid hyperthermia. European Journal of Nanomedicine, 5(1), 11-21.
11. Patel, K., Raj, B. S., Chen, Y. and Lou, X. (2019). Novel theranostic approaches for cancer management: Combining diagnostic and therapeutic capabilities in nanomedicine. Advanced Therapeutics, 2(12), 1900126.
12. Ramanathan, S., Archunan, G., Sivakumar, M., Tamil Selvan, S., Fred, A. L., Kumar, S., Gulyás, B. and Padmanabhan, P. (2018). Theranostic applications of nanoparticles in neurodegenerative disorders. International Journal of Nanomedicine, 13, 5561-5576.

GYANBODH
An International Multidisciplinary Peer Reviewed Journal
ISSN:3048-9792
Volume: 3
Issue: 3
May - June: 2026

13. Siegel, R. L., Miller, K. D., Fuchs, H. E. and Jemal, A. (2021). Cancer Statistics, 2021. CA: A Cancer Journal for Clinicians, 71(1), 7-33.
14. Singh, D., McMillan, J. M., Kabanov, A. V., Sokolsky-Papkov, M. and Gendelman, H. E. (2020). Bench-to-bedside translation of magnetic nanoparticles. Nanomedicine, 15(9), 933-953.
15. Tran, V. A., Lee, S. W., Nguyen, D. C., Kim, J. H., Lee, S. H., Park, K. D. and Vu, N. K. (2020). Folic acid-targeted and pH-responsive drug delivery system based on iron oxide nanoparticles for cancer treatment. Journal of Materials Science, 55(19), 8018-8033.
16. Wang, Y. X. J. (2011). Superparamagnetic iron oxide based MRI contrast agents: Current status of clinical application. Quantitative Imaging in Medicine and Surgery, 1(1), 35-40.
17. Wu, L., Mendoza-Garcia, A., Li, Q. and Sun, S. (2019). Organic phase syntheses of magnetic nanoparticles and their applications. Chemical Reviews, 119(13), 6319-6406.
18. Wu, W., Wu, Z., Yu, T., Jiang, C. and Kim, W. S. (2015). Recent progress on magnetic iron oxide nanoparticles: Synthesis, surface functional strategies and biomedical applications. Science and Technology of Advanced Materials, 16(2), 023501.
19. Xie, J., Liu, G., Eden, H. S., Ai, H. and Chen, X. (2011). Surface-engineered magnetic nanoparticle platforms for cancer imaging and therapy. Accounts of Chemical Research,44(10), 883-892.
20. Yang, X., Yang, M., Pang, B., Vara, M. and Xia, Y. (2015). Gold nanomaterials at work in biomedicine. Chemical Reviews, 115(19), 10410-10488.
21. Zhang, L., Xia, K., Lu, Z., Li, G., Chen, J., Deng, Y., Li, S. and Zhou, F. (2016). Efficient and facile synthesis of gold nanorods with finely tunable plasmonic peaks from visible to near-IR range. Chemistry of Materials, 26(5), 1794-1798.
22. Zhou, Z., Yang, L., Gao, J. and Chen, X. (2019). Structure-relaxivity relationships of magnetic nanoparticles for magnetic resonance imaging. Advanced Materials, 31(8), 1804567.